

# The Role of Small-Scale Topography in Turbulent Mixing of the Global Ocean

Eric Kunze

University of Washington • Seattle, Washington USA

Stefan G. Llewellyn Smith

University of California San Diego • La Jolla, California USA

## Perspective

Maintenance of the observed basin-scale thermohaline (temperature  $T$  and salinity  $S$ ) structure of the world's oceans appears to require mixing to provide dense abyssal waters, which are formed at high latitudes, a pathway back to the surface (Munk and Wunsch, 1998). Small-scale bottom roughness affects mixing processes in the ocean through drag on sinking outflow plumes and abyssal currents on topographic length scales of 0.2-10 km, and through critical reflection (10-100 km) and scattering (0.1-1 km) of internal wave energy to short length scales where it can be lost to turbulent dissipation and mixing. Thus, to understand the thermohaline structure of the oceans, as well as the meridional thermohaline circulation, we must understand the role of turbulent mixing on ocean circulation. This, in turn, requires better-resolved global bathymetry than presently available.

## Life of a Water Parcel

Bathymetry impacts the evolution of a water parcel from its formation as deep and bottom water, its sinking into the abyssal ocean, and its return path to the surface through what is called the meridional thermohaline circulation or global conveyor belt. The formation of dense bottom and deep water on shallow shelves and in marginal seas may be preconditioned by topography, preferentially occurring on shoals or banks. Bottom and deep waters descend into the deep ocean in underwater streams, called outflow plumes, along continental slopes (Figure 1; Price and Baringer, 1994). The degree to which these sink and mix with ambient waters depends sensitively on the steepness of the bottom slope that they hug. As these waters flow along the slopes in a balance between pressure gradients, Coriolis force and Reynolds-stress, they can also spin off to form isolated eddies at abrupt changes in topography as observed off Cape St. Vincent southwest of Portugal (Serra et al., 2002; Bower et al., 1997). The resulting Meddies mix with surrounding waters through lateral double-diffusive intrusions (Hebert et al., 1990) and collisions with seamounts (Richardson et al., 1989).

Waters reaching the deepest parts of the open ocean form bottom waters. These navigate the world's oceans in  $O(10 \text{ cm/s})$  deep western boundary currents that are susceptible to bathymetry encountered along their journey (see the discussion on internal lee waves later). Particularly dramatic mixing occurs as bottom waters spill from one deep basin to another through hydraulically-controlled constrictions (Figure 2; Hogg et al., 1982; Ferron et al., 1998). Bryden and Nurser (2003) go so far as to suggest that mixing of abyssal bottom and overlying waters is dominated by hydraulic flow through constrictive passages. Figure 2 illustrates flow of deep water through a suspected South Atlantic hydraulically controlled fracture zone in the Mid-Atlantic Ridge. Evidence for such a passage comes indirectly through the presence of high-oxygen water from the western basin in the low-oxygen eastern basin. Knowing where the hydraulic control is and whether it is due to vertical or lateral constriction depends on knowing the details of bathymetry (Lawrence, 1990; Wesson and Gregg, 1994). The effect of topography on the flow of currents near the bottom is examined in greater detail in Gille, Metzger and Tokmakian (this issue).

## Mixing is Localized

Our conception of how deep water warms and returns to the surface (or returns to the surface and warms) is in a state of flux with bathymetry potentially playing a large role. A longstanding paradigm has been of slow mixing distributed uniformly through the oceans (Figure 3A; Stommel and Arons 1960; Munk 1966). A simple 1-D vertical advection-diffusion balance implies  $K/w = \rho_z/\rho_{zz}$ . Uniformly distributed upwelling of speed  $w \sim 0.5\text{-}1 \text{ cm day}^{-1}$ , based on the bottom-water formation rate coupled with the observed stratification ratio  $\rho_z/\rho_{zz} \sim 1300 \text{ m}$ , yields an eddy diffusivity  $K \sim O(10^{-4} \text{ m}^2 \text{ s}^{-1})$ . This paradigm has been dispelled by decades of fine-structure and microstructure measurements (e.g., Gregg, 1987; Kunze and Sanford, 1996) and a deliberate tracer-release experiment (Ledwell et al., 1993) that found eddy diffusivities an order of magnitude smaller than predicted

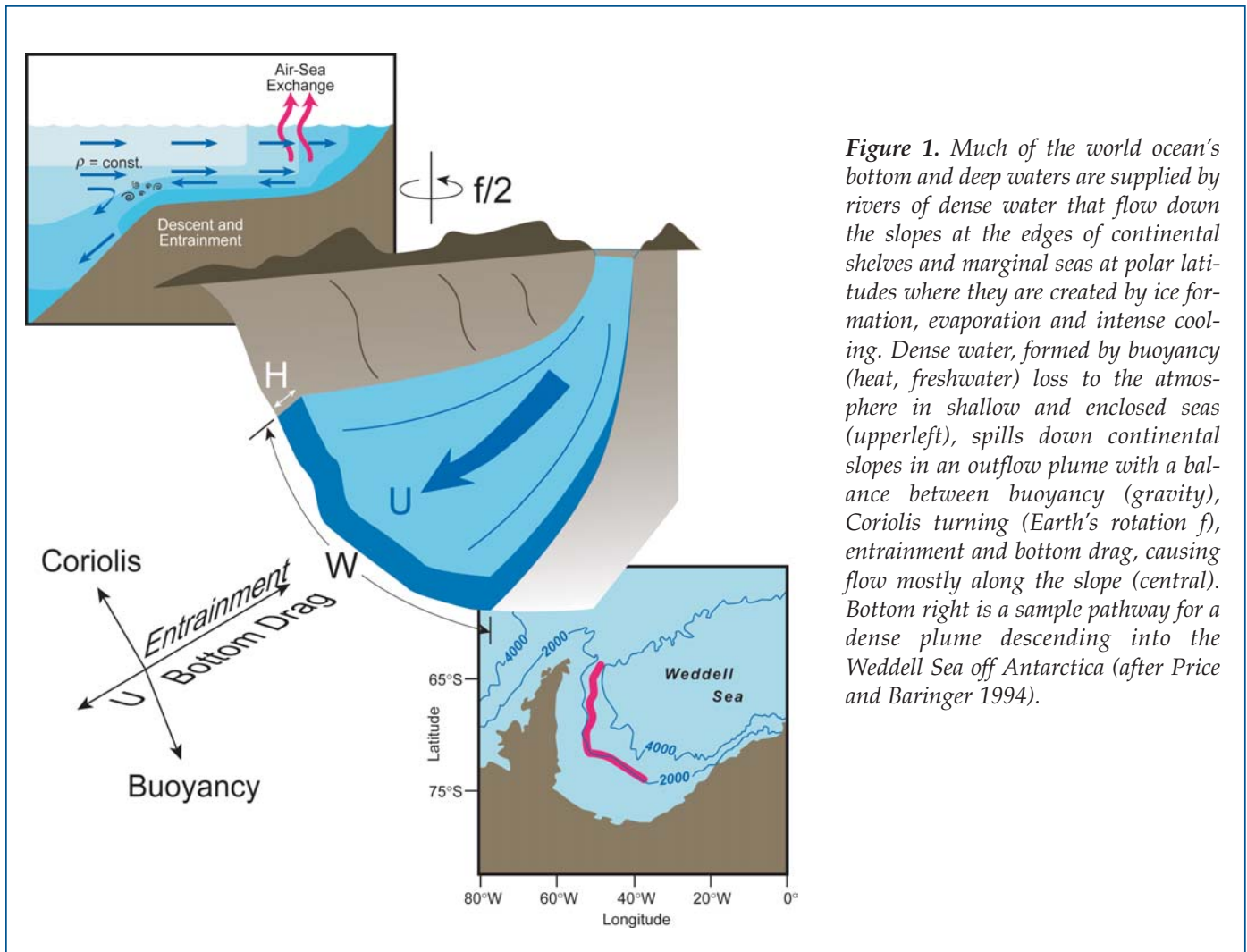


**Figure 1.** Much of the world ocean's bottom and deep waters are supplied by rivers of dense water that flow down the slopes at the edges of continental shelves and marginal seas at polar latitudes where they are created by ice formation, evaporation and intense cooling. Dense water, formed by buoyancy (heat, freshwater) loss to the atmosphere in shallow and enclosed seas (upperleft), spills down continental slopes in an outflow plume with a balance between buoyancy (gravity), Coriolis turning (Earth's rotation  $f$ ), entrainment and bottom drag, causing flow mostly along the slope (central). Bottom right is a sample pathway for a dense plume descending into the Weddell Sea off Antarctica (after Price and Baringer 1994).

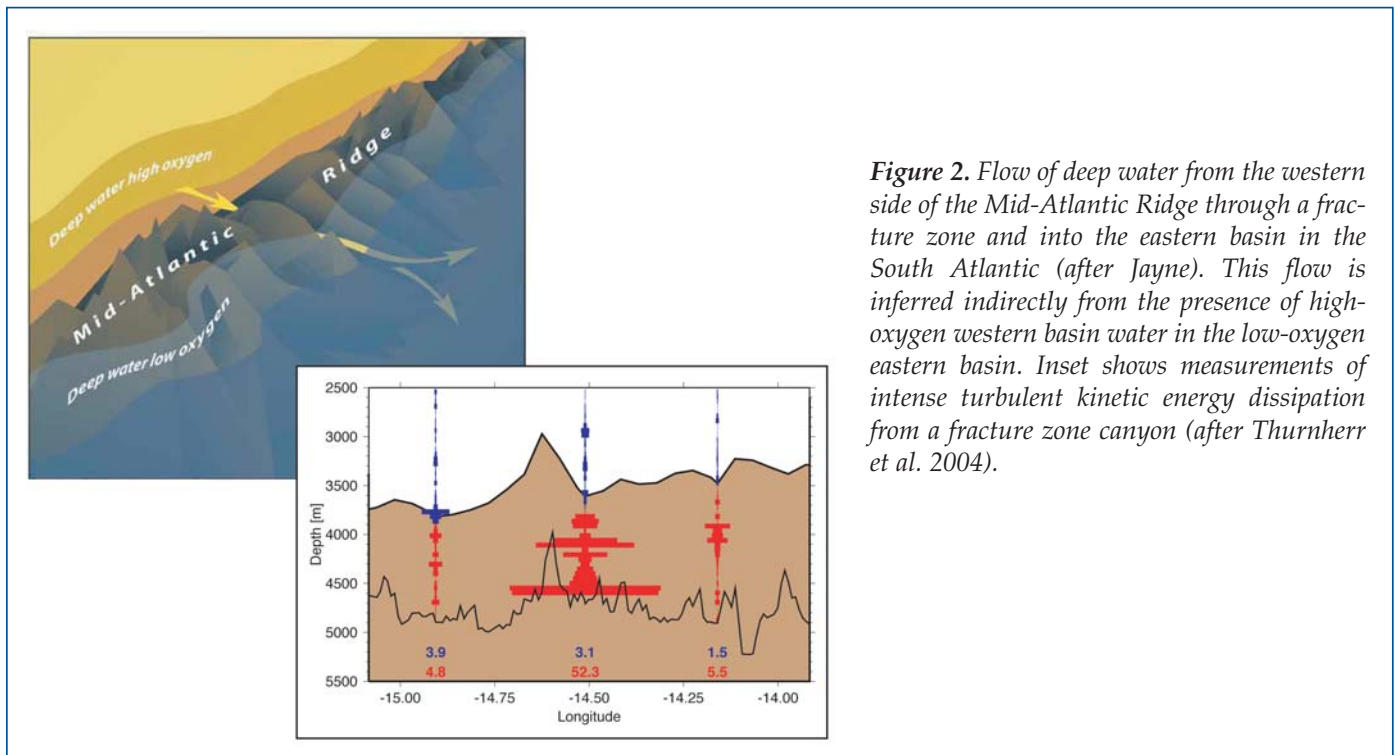


**Figure 2.** Flow of deep water from the western side of the Mid-Atlantic Ridge through a fracture zone and into the eastern basin in the South Atlantic (after Jayne). This flow is inferred indirectly from the presence of high-oxygen western basin water in the low-oxygen eastern basin. Inset shows measurements of intense turbulent kinetic energy dissipation from a fracture zone canyon (after Thurnherr et al. 2004).

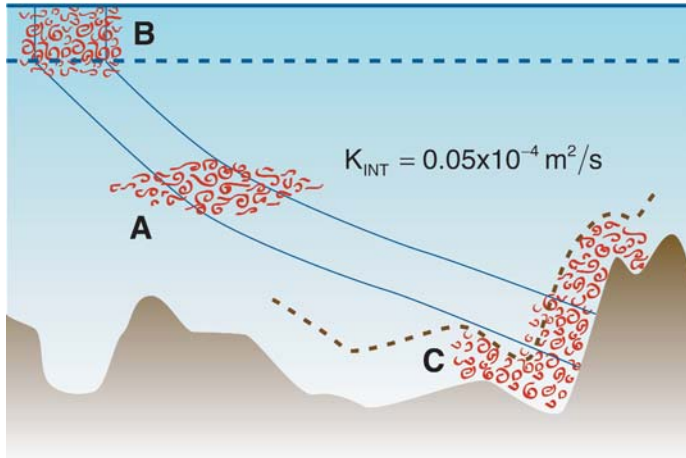
# Abyssal Mixing

## Steady Vertical Advective-Diffusive Balance

$$w \frac{\partial \rho}{\partial z} = - \frac{\partial \langle w' \rho' \rangle}{\partial z} \quad (\text{Munk 1966})$$

$$\Rightarrow \frac{K_e}{w} = \frac{\rho_z}{\rho_{zz}} = 1300 \text{ m} \Rightarrow \langle K_e \rangle \cong 10^{-4} \text{ m}^2/\text{s}$$

for  $w = 1 \text{ cm/day}$  from bottom-water creation



$$\langle w' \rho' \rangle_{\text{TOT}} = \frac{\langle w' \rho' \rangle_A A_A + \langle w' \rho' \rangle_B A_B + \langle w' \rho' \rangle_C A_C}{A_A + A_B + A_C}$$

**Figure 3.** Cartoon illustration of three possible paradigms for ocean mixing. The longstanding hypothesis of uniformly distributed mixing in the ocean interior (A) requires turbulent eddy diffusivities  $K = - \langle w' \rho' \rangle / \bar{\rho}_z$  of  $10^{-4} \text{ m}^2 \text{ s}^{-1}$  while measured values are only  $0.05 \times 10^{-4} \text{ m}^2 \text{ s}^{-1}$ . Alternatives are either surface-enhanced mixing where density surfaces outcrop at polar latitudes (B) or bottom-enhanced mixing over rough topography (C), the products of which then stir along density surfaces to fill the interior.

by the above theory. An important consequence of this is that mixing and upwelling must be strongly localized on boundaries. This implies potentially dramatically shorter time scales for communication of properties between deep and surface waters, which may also have implications for global climate change.

## Boundary Mixing

The lack of mixing in the ocean interior has shifted attention to the boundaries. Several alternative paradigms have emerged. In one, the bulk of the mixing arises from interaction of Ekman transport and eddy stirring across fronts with atmospherically forced mixing in the upper ocean of the Antarctic Circumpolar Current (Figure 3b; e.g., Toggweiler and Samuels, 1993; Gnanadesikan, 1999; Naveira Garabato et al., 2003), though Speer et al. (2000) argue that this is at odds with the sign of air-sea buoyancy-flux. Alternatively, as discussed by Munk and Wunsch (1998), mixing could be concentrated on lateral boundaries (Figure 3c) through a variety of flow/topography interactions. Elevated eddy diffusivities  $K$  are found over the rough bathymetry of the Mid-Atlantic Ridge as compared to

the smoother topography in the central and western Brazil Basin (Figure 4). For further progress to be made in understanding ocean mixing, we need to identify which mechanisms dominate and where. Boundary-mixed waters at turbulent hotspots would spread along density surfaces to set the stratification in the ocean interior (McPhee-Shaw and Kunze, 2002).

## Internal Waves and Mixing

A dominant source of turbulence in the stratified ocean is the breaking of short-vertical-wavelength, near-inertial internal waves with shear exceeding twice the stratification.

$$\left| \frac{\partial(u,v)}{\partial z} \right| > 2N$$

(Box 1) Energy is put into the internal wave field at large vertical scales (low modes) by the wind (Alford, 2003) and tide-topography interactions (Egbert and Ray, 2001; Ray and Mitchum, 1997; Simmons et al., 2004). In contrast to the atmosphere (Fritts and

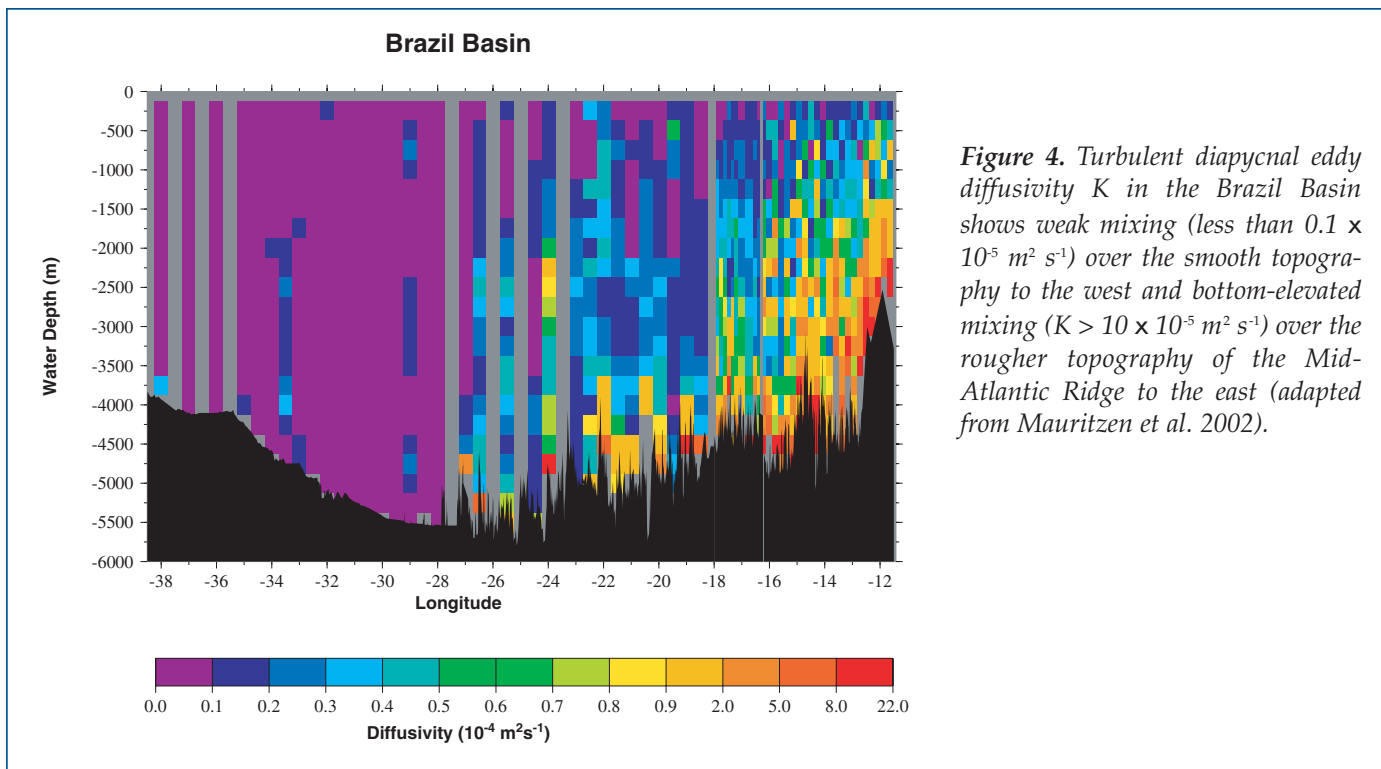


*Figure 4. Turbulent diapycnal eddy diffusivity  $K$  in the Brazil Basin shows weak mixing (less than  $0.1 \times 10^{-5} \text{ m}^2 \text{ s}^{-1}$ ) over the smooth topography to the west and bottom-elevated mixing ( $K > 10 \times 10^{-5} \text{ m}^2 \text{ s}^{-1}$ ) over the rougher topography of the Mid-Atlantic Ridge to the east (adapted from Mauritzen et al. 2002).*

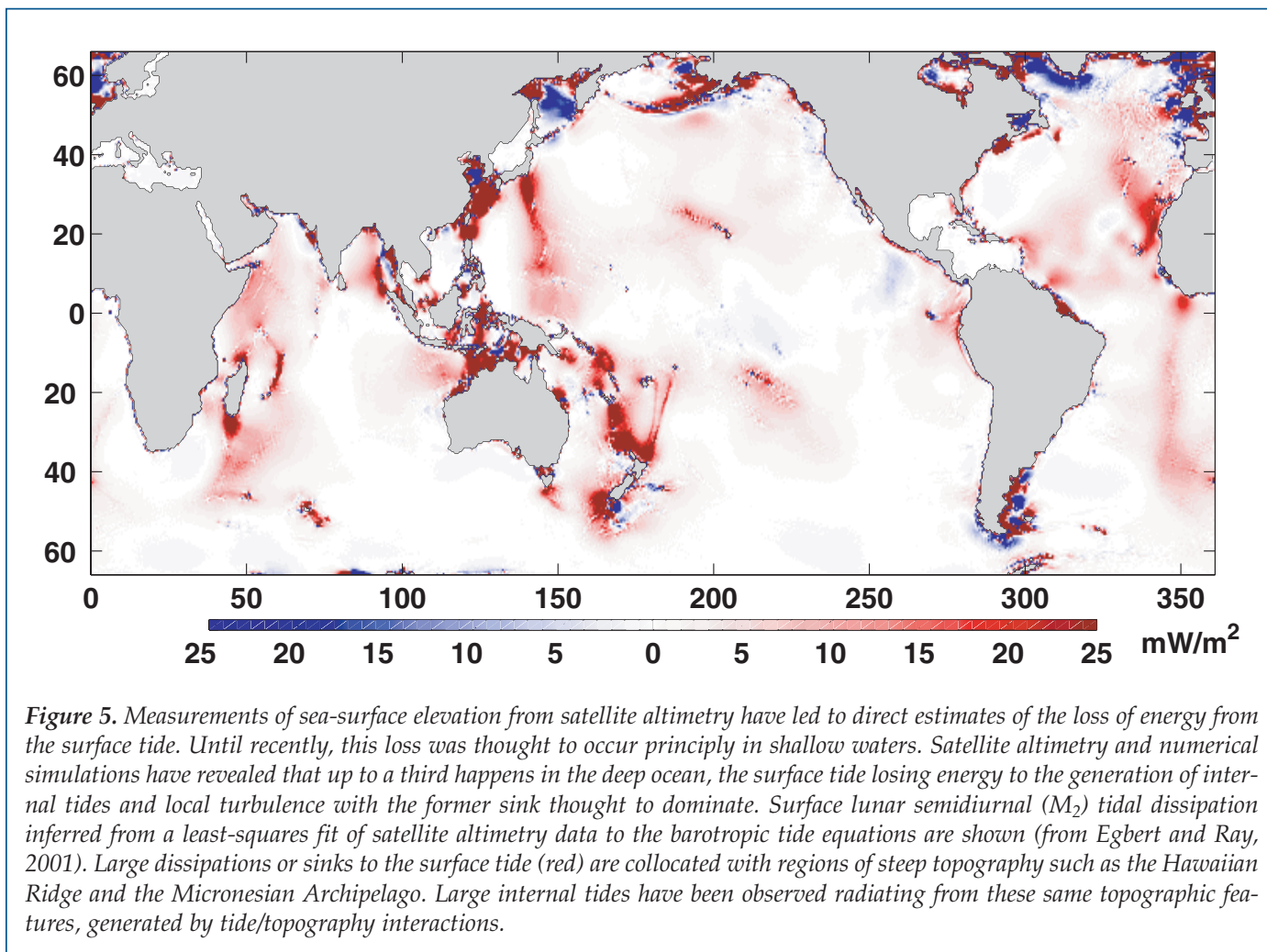


*Figure 5. Measurements of sea-surface elevation from satellite altimetry have led to direct estimates of the loss of energy from the surface tide. Until recently, this loss was thought to occur principally in shallow waters. Satellite altimetry and numerical simulations have revealed that up to a third happens in the deep ocean, the surface tide losing energy to the generation of internal tides and local turbulence with the former sink thought to dominate. Surface lunar semidiurnal ( $M_2$ ) tidal dissipation inferred from a least-squares fit of satellite altimetry data to the barotropic tide equations are shown (from Egbert and Ray, 2001). Large dissipations or sinks to the surface tide (red) are collocated with regions of steep topography such as the Hawaiian Ridge and the Micronesian Archipelago. Large internal tides have been observed radiating from these same topographic features, generated by tide/topography interactions.*

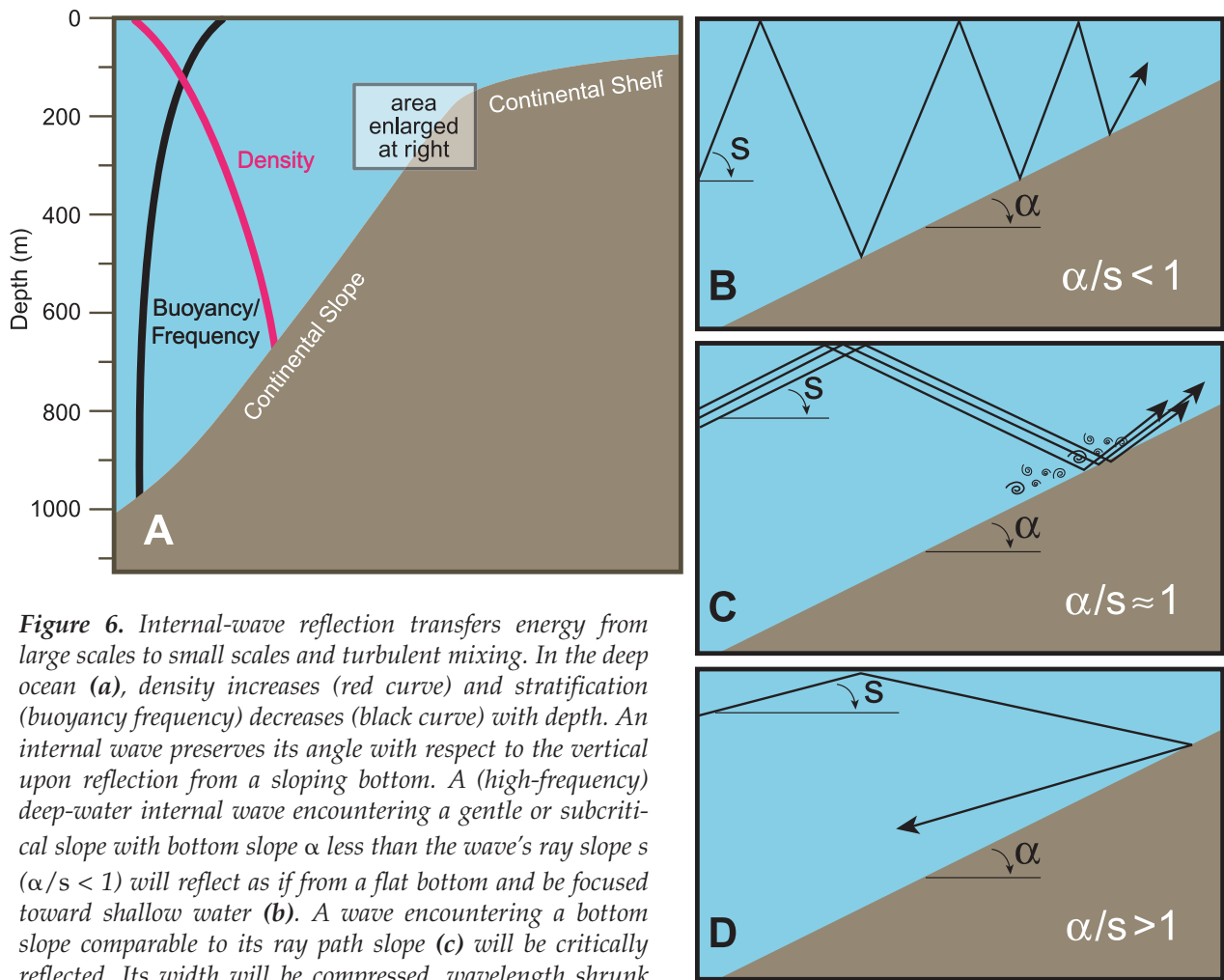


**Figure 6.** Internal-wave reflection transfers energy from large scales to small scales and turbulent mixing. In the deep ocean (a), density increases (red curve) and stratification (buoyancy frequency) decreases (black curve) with depth. An internal wave preserves its angle with respect to the vertical upon reflection from a sloping bottom. A (high-frequency) deep-water internal wave encountering a gentle or subcritical slope with bottom slope  $\alpha$  less than the wave's ray slope  $s$  ( $\alpha/s < 1$ ) will reflect as if from a flat bottom and be focused toward shallow water (b). A wave encountering a bottom slope comparable to its ray path slope (c) will be critically reflected. Its width will be compressed, wavelength shrunk and energy amplified upon reflection, leading to turbulence and mixing. A low-frequency wave will encounter a steep or supercritical slope ( $\alpha/s > 1$ ) and be reflected offshore (d) (after Cacchione et al., 2002).

Alexander, 2003), there is little observational evidence for internal wave generation by convection or lee-wave formation in the ocean. Munk and Wunsch (1998) argue that there is sufficient energy input from deep-ocean tidal and wind forcing to produce the canonical abyssal mixing of  $O(10^{-4} \text{ m}^2 \text{ s}^{-1})$ , with about half coming from each source. These low-mode waves can propagate thousands of kilometers to fill the ocean basins. Energy is transferred to small scales through nonlinear wave-wave interactions and through a variety of interactions with bottom topography. Topographic interactions include (i) internal lee wave generation, (ii) internal tide generation, (iii) internal-wave critical reflection and (iv) internal-wave scattering.

We now describe the various flow-topography interaction mechanisms that could contribute to turbulent mixing, starting with internal lee wave generation.

#### Lee Wave Generation

Subinertial (geostrophic) flow with speed  $U$  over small-scale topography of wavelength  $\lambda$  ( $= 2\pi/k$  where  $k$  is the horizontal wavenumber in radians per meter) will generate internal waves termed lee waves if the flow period  $P \gg \lambda/U$  and  $P_f > \lambda/U > P_N$ , where  $P_f$  and  $P_N$  are the Coriolis and buoyancy periods (see box). For flow speeds  $U = 1 \text{ cm/s}$  ( $10 \text{ cm/s}$ ) typical of central gyre abyssal eddies (deep western boundary currents), this can occur for topographic wavelengths of 0.02 - 1 km (0.5-10 km) (see Figure 7). For corrugations on a slope, the upper-bound wavelength is slightly reduced (MacCready and Pawlak, 2001). In this range of corrugation scales, internal waves radiate energy and momentum into the overlying water, and can break to produce turbulent mixing. At larger and smaller topographic wavelengths, a forced bottom-trapped

## Box 1

### Internal Gravity Waves in the Ocean

Internal gravity waves are allowed by the stratification of the ocean interior (e.g., Lighthill 1979), which provides a gravitational force to restore a water parcel to its equilibrium depth if it is displaced. Inertia causes the restoration to overshoot, giving rise to waves. These internal waves exist between the Coriolis period  $P_f$  ( $= 12 \text{ h}/\sin(\text{latitude})$ ) and the buoyancy period  $P_N$  ( $= 0.5\text{-}3 \text{ h}$ ) with most energy being at Coriolis and tidal periods. They also have variance at vertical wavelengths ranging from the largest vertical scale that will fit in the ocean depth (mode one) to roughly 10 m, with most energy and energy-flux at large scales and most shear and strain at small scales. The distribution (spectrum) of wave energy with respect to frequency  $\omega = 2\pi/P$  and wavelength  $\lambda$  is almost universal in the ocean, and is described by the Garrett and Munk (GM76) model spectrum (though GM76 doesn't include the more-variable tidal contributions). These waves propagate vertically as well as horizontally, with the vertical energy propagation in the opposite sense to the vertical phase propagation.

response occurs; except very near the above limits, the response is effectively barotropic. The generation of mountain lee waves that propagate upward to deposit their momentum at higher altitudes is an important process for the atmospheric mean circulation but oceanic geostrophic flows tend to flow around rather than over topography and there is little observational evidence for this mechanism in the ocean.

#### *Tide/Topography Generation of Internal Tides*

Away from deep western boundary currents and constricted passages, the strongest currents in abyssal waters are associated with surface tidal currents, dominantly the lunar semidiurnal ( $M_2$ ) tide. Semidiurnal barotropic currents will interact with topography on horizontal wavelengths smaller than about  $(f_{30}/f) \times 150 \text{ km}$  to produce internal waves at latitudes less than  $75.4^\circ$  (e.g., Bell, 1975; Baines, 1982); diurnal internal waves are confined to latitudes less than  $30^\circ$ . Three non-dimensional parameters control the nature of the internal response (St. Laurent and Garrett, 2002): the ratio of topography height to water depth  $h/H$ , the ratio of topographic to wave characteristic slope,

$$\alpha/s = \nabla h / \sqrt{(\omega^2 - f^2) / (N^2 - \omega^2)}$$

and the ratio of tidal excursion to topographic length scale  $\chi/\ell = kU/\omega$ . For small tidal excursion compared

to the topography length scale  $\ell$  ( $=\lambda/2\pi = k^{-1}$ ), the response is linear and has the same frequency as the forcing. For gentle (subcritical,  $\alpha/s < 1$ ) bottom slopes and small-amplitude topography, internal tide generation can be deduced spectrally:  $S[w](k) = U^2 k^2 S[h](k)$  (Bell 1975) where  $S[h](k)$  is the horizontal wavenumber spectrum of the topography  $h(x, y)$  and  $S[w](k)$  the internal tide vertical velocity response. The vertical wavenumber can be deduced from the dispersion relation. As topography becomes steeper (supercritical,  $\alpha/s > 1$ ) and taller, numerical (Merrifield et al., 2001) or more complicated analytical (Baines, 1982; St. Laurent et al., 2003; Petrelis et al., 2004) techniques must be used.

Satellite altimetry has shown that roughly one third of the surface tidal dissipation (800 GW) occurs in the deep ocean (Figure 5; Egbert and Ray, 2001) and is associated with steep tall topography from which internal tides are observed to radiate (Ray and Mitchum, 1996). A global baroclinic numerical model (Simmons et al., 2004) finds that 75% of the deep-ocean tidal dissipation occurs at only 20 sites of abrupt topography. In contrast, the Mid-Atlantic Ridge and other mid-ocean ridges, which are characterized by subcritical ( $\alpha/s < 1$ ) though complicated topography, only contribute significantly to tidal dissipation because they are so widespread. We note that shelf breaks, despite having topography favorable for internal tide generation, are not major generators of internal tides because, with some notable exceptions like the Bay of Biscay (Pingree and New, 1989) and the Queen Charlotte Islands (Cummins and Oey, 1997), tidal currents are largely along rather than across the shelf break (Sjöberg and Stigebrandt, 1992). In shallow water over abrupt topography, nonlinearity becomes more important as the tidal excursion exceeds the topographic scale, forming harmonics and ultimately solibores.

The bulk of the surface tidal loss from these abrupt topographic features appears to radiate away as internal waves (Althaus et al., 2003; Rudnick et al., 2003) with only a small fraction lost locally to turbulence. The fate of this energy, as well as that of the rest of the ubiquitous internal wave field, depends in part on topography. There are two mechanisms that can transfer internal wave energy toward smaller scales and turbulent dissipation/mixing: critical reflection and scattering.

#### *Critical Reflection*

Internal waves do not obey Snell's law; they preserve their angle  $s$  with respect to the vertical rather than the boundary when they reflect (Phillips, 1966). An internal wave reflecting from a steep (supercritical) slope will reflect horizontally, as if from a vertical wall (Figure 6b). A wave reflecting from a gentle (subcritical) slope will reflect vertically (Figure 6d). Most interestingly, an internal wave encountering a bottom slope  $\alpha$

comparable to its ray-path (characteristic) slope  $s$  will be critically reflected to a much smaller wavelength and much higher amplitude (Figure 6c; Eriksen, 1982; Slinn and Riley, 1996). The wave's energy will be amplified and its progress slowed so that it is certain to break to produce turbulence (Garrett and Gilbert, 1987). Abyssal basins are subcritical (gentle) for all but near-inertial frequencies. Because abyssal stratification is weak, only very steep (often isolated) topographic features are near critical at semidiurnal tidal periods. Much of the world's continental slope is nearly critical for semidiurnal periods, making the slope a potential sink for internal tides (Figure 6A). In fact, continental slope morphology may be controlled by the internal tide (Cacchione et al., 2002).

The peculiar reflection properties of internal waves also allow trapping and focusing by a shoaling bottom. Deep-ocean waves with ray slopes  $s$  exceeding the bottom slope  $\alpha$  will be reflected upslope (Wunsch, 1969). As the water depth decreases, these waves will be increasingly amplified, likely leading to turbulence. Evidence for this focusing was recently found in Monterey Submarine Canyon (Kunze et al., 2002) where turbulent mixing was as strong as in hydraulically controlled flows (Carter and Gregg, 2002).

#### Internal Wave Scattering

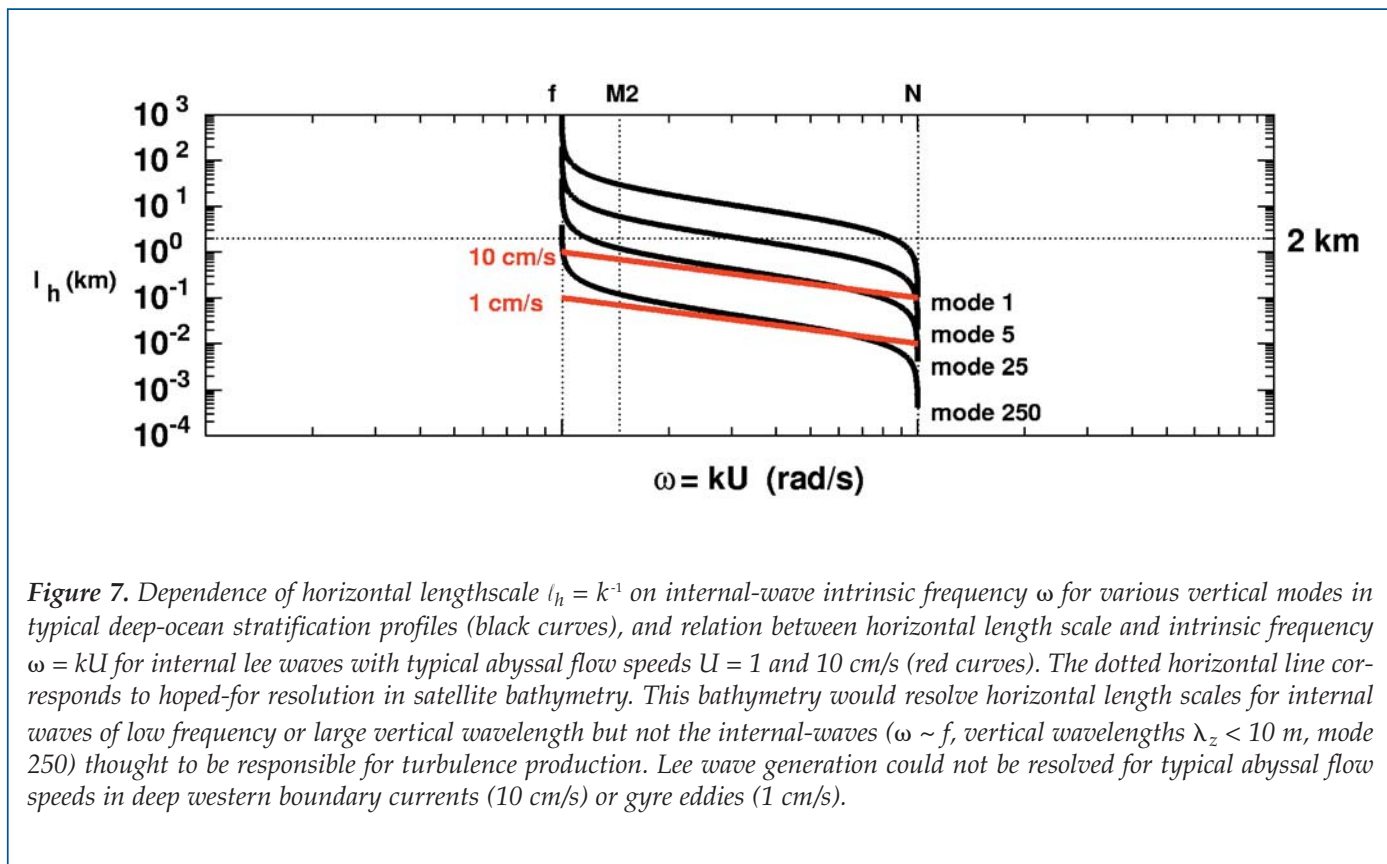
An internal wave encountering bottom topography with length scales smaller than those of the wave

will have much of its energy scattered into the scales of the topography. As in the case of tidal interaction with topography, this process is linear in wave amplitude but nonlinear in bottom height so that, if the bottom height and slope are sufficiently small ( $h \ll H, \alpha \ll s$ ), the scattered wave field can be computed in terms of Fourier components of the bottom topography (Müller and Xu, 1992). Scattering redistributes energy from large to small length scales. These theories have not been applied to recent topographic models (e.g., Goff and Jordan, 1988). However, they are also only marginally valid for oceanographic conditions as the requirement for small topographic slope breaks down for near-inertial waves. Recent measurements over a corrugated continental slope find that critical reflection rather than scattering is the dominant mechanism of transferring low-mode internal wave energy to small scales and turbulent mixing (Nash et al., 2004).

#### Summary

Evidence increasingly points to the importance of mixing in controlling the ocean's global conveyor belt, but it is as yet unclear whether the surface or bottom boundary is contributing the most mixing.

A number of flow/topography mechanisms could be contributing significantly to turbulent mixing near the bottom, including outflow plume descent down continental slopes, hydraulic flow through constricted passages, internal lee wave generation, internal tide



generation, internal wave critical reflection and scattering. Again, it is unclear which mechanisms are most important. Improved global bathymetry would make an important contribution to sorting out the relative roles of these mechanisms by, for example, better identifying the depth and width of passages between deep basins for hydraulic flow and the steepness of the continental slope for descending plumes of dense water. Extant satellite bathymetry (Smith and Sandwell, 1997) has already contributed to better siting and designing of shipboard field programs and has been successfully used to estimate dissipation of the surface tide generation of the lowest-vertical-mode (which carry most of the energy-flux) internal tides by tide-topography interactions at steep localized topographic features (Simmons et al. 2004; Merrifield et al., 2001). Perhaps the most efficient means of transferring energy from large vertical scales in the internal wave field to the small scales responsible for turbulence production is critical reflection where the bottom slope is the same as the slope of the ray path (Eriksen, 1982). Since the energy- and flux-containing internal waves have wavelengths of O(100 km) and larger (Figure 7), and the critical reflection process seems indifferent to smaller-scale topography (Nash et al. 2004), resolving topographic wavelengths of 50-100 km may be sufficient to quantify this process.

Other processes such as lee wave generation and internal wave scattering (Figure 7) require direct transfer of energy to small vertical scales, and so require correspondingly small horizontal scales (1 km) so that satellite bathymetry will never provide sufficient resolution. Where the statistics of finer-scale bathymetry can be inferred from satellite-inferred bathymetry (Goff and Jordan, 1988), these processes might still be quantified, as well as the generation of smaller-vertical-scale internal tides. However, these processes may also be less important. Because subinertial abyssal flows tend to be weak and to go around rather than over topography, internal lee wave generation can only occur for topographic scales of 0.02-10 km (Figure 7). Lee wave generation is likely to be confined to the narrow deep western boundary currents and Antarctic Circumpolar Currents, and so may not be globally significant.

Scattering of larger waves to the O(10 m) vertical wavelengths (mode 250) that produce turbulence requires resolving topographic wavelengths of 0.1-1 km (Figure 7). However, there is little observational support for this process being important in the ocean.

Thus, modest improvements to existing global bathymetry may be sufficient to improve estimates of mixing associated with topography in the world's oceans. Regions such as canyons and passages with intense mixing due to nonlinear processes can be identified, while the spectral characteristics of large, smoother regions associated with wave transformation, leading later to mixing, can be calculated. 

## Acknowledgments

We are grateful to Sarah Gille, Peter Haynes, Steve Jayne, Lou St. Laurent and Bill Young for helpful suggestions. Some of this material was presented at the Workshop on Ocean Circulation, Bathymetry and Climate held at Scripps Institute of Oceanography during October 2002. Support from NASA Goddard Grant NAG5-12388 for Stefan Llewellyn Smith and from NSF Grant No. OCE 99-06731 for Eric Kunze are acknowledged.

## References

- Althaus, A.M., E. Kunze, and T.B. Sanford, 2003: Internal tide radiation from Mendocino Escarpment. *J. Phys. Oceanogr.*, 33, 1510-1527.
- Baines, P.G., 1982: On internal tide generation models. *Deep-Sea. Res.*, 29, 307-338.
- Bell, T.H., 1975: Topographically-generated internal waves in the open ocean. *J. Geophys. Res.*, 80, 320-327.
- Bower, A., L. Armi, and I. Ambar, 1997: Lagrangian observations of Meddy formation during a Mediterranean Undercurrent Seeding Experiment. *J. Phys. Oceanogr.*, 27, 2545-2575.
- Bryden, H.L., and A.J.G. Nurser, 2003: Effects of strait mixing on ocean stratification. *J. Phys. Oceanogr.*, 33, 1870-1872.
- Cacchione, D.A., L.F. Pratson, and A.S. Ogston, 2002: The shaping of continental slopes by internal tides. *Science*, 296, 724-727.
- Carter, G.S., and M.C. Gregg, 2002: Intense variable mixing near the head of Monterey Submarine Canyon. *J. Phys. Oceanogr.*, 32, 3145-3165.
- Cummins, P.F., and L. Oey, 1997: Simulation of barotropic and baroclinic tides off northern British Columbia. *J. Phys. Oceanogr.*, 27, 762-781.
- Egbert, G.D., and R. Ray, 2001: Estimates of  $M_2$  tidal energy dissipation from TOPEX/POSEIDON altimeter data. *J. Geophys. Res.*, 106, 22,475-22,502.
- Eriksen, C.C., 1982: Observations of internal wave reflection off sloping bottoms. *J. Geophys. Res.*, 87, 525-538.
- Ferron, B., H. Mercier, K. Speer, A. Gargett, and K. Polzin, 1998: Mixing in the Romanche Fracture Zone. *J. Phys. Oceanogr.*, 28, 1929-1945.
- Fritts, D.C., and M.J. Alexander, 2003: Gravity-wave dynamics and effects in the middle atmosphere. *Rev. Geophys.*, 41, DOI: 10.1029/2001RG000106.
- Garrett, C., and D. Gilbert, 1988: Estimates of vertical mixing by internal waves reflected off a sloping bottom. Pp. 405-423 in *Smallscale Turbulence and Mixing in the Ocean*, J.C.J. Nihoul and B.M. Jamart, eds., Elsevier.
- Gnanadesikan, A., 1999: A simple predictive model for the structure of the oceanic pycnocline. *Science*, 283, 2077-2079.
- Goff, J.A., and T.H. Jordan, 1988: Stochastic modelling

- of seafloor morphology: Inversion of Sea Beam data for 2nd-order statistics. *J. Geophys. Res.*, 93, 13,589-13,608.
- Gregg, M.C., 1987: Diapycnal mixing in the thermocline: A review. *J. Geophys. Res.*, 92, 5249-5286.
- Hebert, D., N. Oakey, and B. Ruddick, 1990: Evolution of a Mediterranean salt lens: Scalar properties. *J. Phys. Oceanogr.*, 20, 1468-1483.
- Hogg, N., P. Biscaye, W. Gardner, and W.J. Schmitz Jr., 1982: On the transport and modification of Antarctic Bottom Water in the Vema Channel. *J. Mar. Res.*, 40 (Suppl.), 231-263.
- Klymak, J.M., and M.C. Gregg, 2004: Tidally-generated turbulence and mixing over the Knight Inlet sill. *J. Phys. Oceanogr.*, submitted.
- Kunze, E., and T.B. Sanford, 1996: Abyssal mixing: Where it isn't. *J. Phys. Oceanogr.*, 26, 2286-2296.
- Kunze, E., L.K. Rosenfeld, G.S. Carter, and M.C. Gregg, 2002: Internal waves in Monterey Submarine Canyon. *J. Phys. Oceanogr.*, 32, 1890-1913.
- Lawrence, G.A., 1990: On the hydraulics of Boussinesq and non-Boussinesq two-layer flows. *J. Fluid Mech.*, 215, 457-480.
- Ledwell, J.R., A.J. Watson, and C.S. Law, 1993: Evidence of slow mixing across the pycnocline from an open-ocean tracer-release experiment. *Nature*, 364, 701-703.
- Llewellyn Smith, S.G., and W.R. Young, 2002: Conversion of the barotropic tide. *J. Phys. Oceanogr.*, 32, 1554-1566.
- Llewellyn Smith, S.G., and W.R. Young, 2003: Tidal conversion at a very steep ridge. *J. Fluid Mech.*, 495, 175-191.
- MacCready, P., and G. Pawlak, 2001: Stratified flow along a rough slope: Separation drag and wave drag. *J. Phys. Oceanogr.*, 31, 2824-2839.
- Mauritzen, C., K.L. Polzin, M.S. McCartney, R.C. Millard, and D.E. West-Mack, 2002: Evidence in hydrography and density finestructure for enhanced vertical mixing over the Mid-Atlantic Ridge. *J. Geophys. Res.*, 107, 10.1019/2001JC000801.
- McPhee-Shaw, E.E., and E. Kunze, 2003: Boundary-layer intrusions from a sloping bottom: A mechanism for generating intermediate nepheloid layers. *J. Geophys. Res.*, 107, 10.1029/2001JC000801.
- Merrifield, M.A., P.E. Holloway, and T.S. Johnston, 2001: The generation of internal tides at the Hawaiian Ridge. *J. Geophys. Res.*, 106, 559-562.
- Müller, P., and N. Xu, 1992: Scattering of oceanic internal gravity waves off random bottom topography. *J. Phys. Oceanogr.*, 22, 474-488.
- Munk, W., 1966: Abyssal recipes. *Deep-Sea Res.*, 13, 707-730.
- Munk, W., and C. Wunsch, 1998: Abyssal recipes II: Energetics of tidal and wind forcing. *Deep-Sea Res.*, 45, 1977-2010.
- Nash, J.D., and J.N. Moum, 2001: Internal hydraulic flows in the continental shelf: High drag states over a small bank. *J. Geophys. Res.*, 106, 4593-4611.
- Nash, J.D., E. Kunze, J.M. Toole, and R.W. Schmitt, 2004: Internal tide reflection and turbulent mixing on the continental slope. *J. Phys. Oceanogr.*, 34, in press.
- Naveira Garabato, A.C., D.P. Stevens, and K.J. Heywood, 2003: Water-mass conversion, fluxes and mixing in the Scotia Sea diagnosed by an inverse model. *J. Phys. Oceanogr.*, 33, 2565-2587.
- Petrelis, F., S.G. Llewellyn Smith, and W.R. Young, 2004: Tidal conversion at a submarine ridge. *J. Phys. Oceanogr.*, submitted.
- Phillips, O.M., 1966: *The Dynamics of the Upper Ocean*. Cambridge University Press, New York, 336 pp.
- Pingree, R.D., and A.L. New, 1989: Downward propagation of internal tidal energy into the Bay of Biscay. *Deep-Sea Res.*, 36, 735-758.
- Price, J.F., and M. O'Neil Baringer, 1994: Outflows and deep-water production by marginal seas. *Prog. Oceanogr.*, 33, 161-200.
- Ray, R.D., and G.T. Mitchum, 1997: Surface manifestation of internal tides in the deep ocean: Observations from altimetry and island gauges. *Prog. Oceanogr.*, 40, 135-162.
- Richardson, P.L., D. Walsh, L. Armi, M. Schröder, and J.F. Price, 1989: Tracking three Meddies with SOFAR floats. *J. Phys. Oceanogr.*, 19, 371-383.
- Rudnick, D.L., T.J. Boyd, R.E. Brainard, G.S. Carter, G.D. Egbert, M.C. Gregg, P.E. Holloway, J.M. Klymak, E. Kunze, C.M. Lee, M.D. Levine, D.S. Luther, J.P. Martin, M.A. Merrifield, J.N. Moum, J.D. Nash, R. Pinkel, L. Rainville, and T.B. Sanford, 2003: From tides to mixing along the Hawaiian Ridge. *Science*, 301, 355-357.
- Serra, N., S. Sadoux, I. Ambar, and D. Renouard, 2002: Observations and laboratory modeling of Meddy generation at Cape St. Vincent. *J. Phys. Oceanogr.*, 32, 3-25.
- Simmons, H.L., R.W. Hallberg, and B.K. Arbic, 2004: Internal wave generation in a global baroclinic tide model. *Deep-Sea Res. II*, submitted.
- Sjöberg, B., and A. Stigebrandt, 1992: Computations of the geographical distribution of the energy-flux to mixing processes via internal tides and the associated vertical circulation in the ocean. *Deep-Sea Res.*, 39, 269-291.
- Slinn, D.N., and J.J. Riley, 1996: Turbulent mixing in the oceanic boundary layer due to internal wave reflection from sloping terrain. *Dyn. Atmos. Oceans*, 23, 51-62.
- Smith, W.H.F., and D.T. Sandwell, 1997: Global seafloor topography from satellite altimetry and ship depth soundings. *Science*, 277, 1956-1962.
- Speer, K., S.R. Rintoul, and B. Sloyan, 2000: The diabatic Deacon cell. *J. Phys. Oceanogr.*, 30, 3212-3222.
- St. Laurent, L.C., and C. Garrett, 2002: The role of internal tides in mixing the deep ocean. *J. Phys. Oceanogr.*, 32, 2882-2899.

- St. Laurent, L.C., S. Stringer, C. Garrett, and D. Perrault-Joncas, 2003: The generation of internal tides at abrupt topography. *Deep-Sea Res.*, 50, 987-1003.
- Stommel, H., and A.B. Arons, 1960: On the abyssal circulation of the world ocean - I. Stationary planetary flow patterns on a sphere. *Deep-Sea Res.*, 6, 140-154.
- Thurnherr, A.M., L.C. St. Laurent, K.G. Speer, J.M. and J.R. Ledwell, 2004: Mixing associated with sills in canyons on the mid-ocean ridge flank. *J. Phys. Oceanogr.*, submitted.
- Toggweiler, J.R., and B. Samuels, 1993: Is the magnitude of the deep outflow from the Atlantic Ocean actually governed by Southern Hemisphere winds? Pp. 303-331 in *The Global Carbon Cycle*. M. Heimann, ed., NATO ASI Series, Springer-Verlag.
- Wesson, J.C., and M.C. Gregg, 1994: Mixing at Camarinal Sill in the Strait of Gibraltar. *J. Geophys. Res.*, 99, 9847-9878.
- Wunsch, C., 1969: Progressive internal waves on slopes. *J. Fluid Mech.*, 35, 131-144.

